Action Potentials and Chemosensitive Conductances in the Dendrites of Olfactory Neurons Suggest New Features for Odor Transduction

ADRIENNE E. DUBIN and VINCENT E. DIONNE

From the Department of Pharmacology, University of California, San Diego, La Jolla, California 92093-0636

ABSTRACT Odors affect the excitability of an olfactory neuron by altering membrane conductances at the ciliated end of a single, long dendrite. One mechanism to increase the sensitivity of olfactory neurons to odorants would be for their dendrites to support action potentials. We show for the first time that isolated olfactory dendrites from the mudpuppy *Necturus maculosus* contain a high density of voltage-activated Na^+ channels and produce Na-dependent action potentials in response to depolarizing current pulses. Furthermore, all required steps in the transduction process beginning with odor detection and culminating with action potential initiation occur in the ciliated dendrite. We have previously shown that odors can modulate Cl^- and K^+ conductances in intact olfactory neurons, producing both excitation and inhibition. Here we show that both conductances are also present in the isolated, ciliated dendrite near the site of odor binding, that they are modulated by odors, and that they affect neuronal excitability. Voltage-activated Cl^- currents blocked by 4,4′-diisothiocyanatostilbene-2,2′ disulfonic acid and niflumic acid were found at greater than five times higher average density in the ciliated dendrite than in the soma, whereas voltage-activated K^+ currents inhibited by intracellular Cs^+ were distributed on average more uniformly throughout the cell. When ciliated, chemosensitive dendrites were stimulated with the odorant taurine, the responses were similar to those seen in intact cells: Cl^- currents were increased in some dendrites, whereas in others Cl^- or K^+ currents were decreased, and responses washed out during whole-cell recording. The Cl^- equilibrium potential for intact neurons bathed in physiological saline was found to be −45 mV using an on-cell voltage-ramp protocol and delayed application of channel blockers. We postulate that transduction of some odors is caused by second messenger-mediated modulation of the resting membrane conductance (as opposed to a specialized generator conductance) in the cilia or apical region of the dendrite, and show how this could alter the firing frequency of olfactory neurons.

Address correspondence to Dr. Vincent E. Dionne, Boston University Marine Program, Marine Biological Laboratory, Woods Hole, MA 02543.

Dr. Dubin's present address is Department of Biology, San Diego State University, San Diego, CA 92182.

J. GEN. PHYSIOL. © The Rockefeller University Press · 0022-1295/94/02/0181/21 $2.00
Volume 103 February 1994 181–201

INTRODUCTION

Odor transduction by olfactory neurons relies on processes that affect one or more types of membrane ion channel. These processes, which alter the electrical activity in individual neurons, occur simultaneously in many receptor cells when an odor is inhaled, producing a pattern of neuronal activity that the brain interprets as smell. The latency between exposure to odors and the initial response appears to be just a few hundred milliseconds (Firestein, Shepherd, and Werblin, 1990), during which odor molecules bind, second messenger pathways are activated, and ion channels are modulated. The rapidity of the overall response suggests that the channels modulated by odors must be located close to the odor receptor sites, probably in the ciliary and/or apical dendritic membranes. This must be characteristic of odor-sensitive conductances (Nakamura and Gold, 1987; Kurahashi, 1989; Lowe and Gold, 1991; Firestein, Zufall, and Shepherd, 1991*b;* Frings, Benz, and Lindemann, 1991; Kleene, 1993). Earlier work suggested that the pathways of odor transduction converged to activate a nonselective cation channel in ciliary and dendritic membranes of olfactory neurons (Nakamura and Gold, 1987; Lowe and Gold, 1991) causing depolarization and neuronal excitation (Nakamura and Gold, 1987; Kolesnikov, Zhainazarov, and Kosolapov, 1990; Miyamoto, Restrepo, and Teeter, 1992; Firestein, Darrow, and Shepherd, 1991*a;* Zufall, Firestein, and Shepherd, 1991). More recent work has implicated a variety of additional conductances that might be modulated by odorants including Na^+ (Pun and Gesteland, 1991; Rajendra, Lynch, and Barry, 1992), K^+ (Maue and Dionne, 1987; Lynch and Barry, 1991; Michel, McClintock, and Ache, 1991; Dionne, 1992; Dubin and Dionne, 1993), Ca^{2+} (Restrepo, Miyamoto, Bryant, and Teeter, 1990; Miyamoto et al., 1992), and Cl^- (McClintock and Ache, 1989; Kleene and Gesteland, 1991; Dubin and Dionne, 1993; Kurahashi and Yau, 1993; Kleene, 1993). It is believed that odor-induced potentials originating at the apical end of the olfactory dendrite propagate passively to the soma to modulate firing of action potentials at the axon hillock (Getchell, 1973; Juge, Holley, and Delaleu, 1979; Getchell, 1986). However, the ability of the dendrite itself to fire action potentials has not been directly tested.

Previously, we showed that odorants can modulate at least three different conductances in mudpuppy olfactory neurons, including a Cl^-, a K^+, and a nonselective cation conductance (Dubin and Dionne, 1993). We have now examined the membrane conductances in isolated, ciliated dendrites from mudpuppy olfactory neurons, testing in particular for the Cl^- and K^+ conductances to determine if they are close to the apical site of odorant action and to evaluate their effects on cell excitability. Not only are these conductances present in the isolated dendrites, but they also retain their odor sensitivity. In addition, the dendrites contain Na^+ channels at high density and can support action potentials. These features suggest that some odors may be transduced by modulating the resting membrane conductance in cilia and the dendritic ending, thus eliciting action potentials locally which propagate the full length of the cell to reach the olfactory bulb.

METHODS

Cells were dissociated from the olfactory epithelia of adult aquatic salamanders (*Necturus maculosus*) without enzymes using a low Ca^{2+} alkaline treatment followed by mechanical disruption (Dionne, 1992; Dubin and Dionne, 1993). The procedure produced large numbers

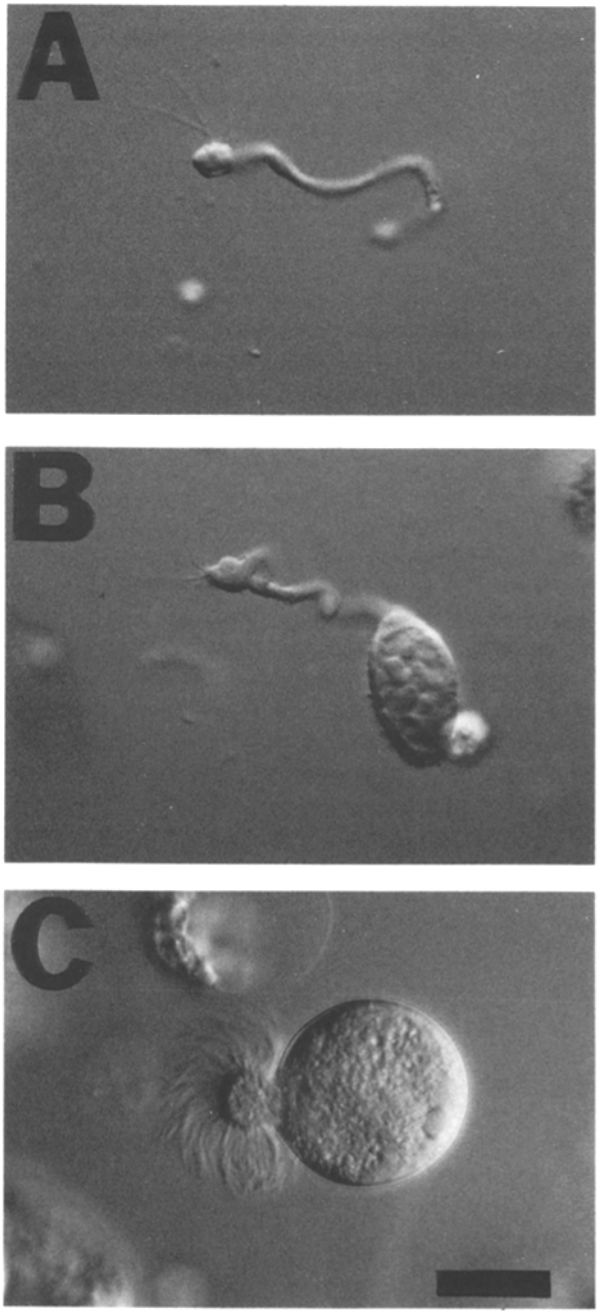

FIGURE 1. Ciliated cells acutely isolated from mudpuppy olfactory epithelium. (*A*) An isolated olfactory dendrite. At least five cilia are visible projecting from the dendritic knob in this plane of focus. There was no indication of a soma or of fragments of somatic membrane at any level of focus. (*B*) An intact olfactory receptor neuron. Mudpuppy olfactory neurons have a large, ovoid soma nearly filled by the nucleus and a single dendrite which ends in a knob and cilia. The axon, which is not visible here, emerges from the cell body opposite the dendrite. A small piece of debris can be seen touching the soma, lower right. (*C*) A non-neuronal Medusa cell. Viable Medusa cells have a tuft of about 100 vigorously beating cilia. Although the corresponding cell type in the intact epithelium is uncertain, these may be sustentacular or respiratory cells whose rapidly beating cilia can be observed in vivo stirring the mucus layer. Medusa cells appear to round up immediately after dissociation. In contrast, olfactory neurons retain their general morphology after isolation, but then slowly swell over the course of several hours. The pictures here were taken ~3 h after dissociation. All photomicrographs were taken at ×500 using a water immersion objective and Nomarski differential interference contrast optics. Scale bar, 20 μM.

of viable neurons, each with 5–20 cilia at the end of a single dendrite but without most of the axon; these are referred to as "intact neurons" (Fig. 1 *B*). In addition, olfactory dendrites complete with cilia but entirely detached from their cell soma were found (Fig. 1 *A*); these are referred to as "isolated dendrites." Intact neurons and isolated dendrites were visually identified at a magnification of 500 using a compound microscope fitted with a ×40

water-immersion objective and high-resolution differential interference contrast optics (Carl Zeiss, Inc., Thornwood, NY). The contrast enhancement afforded by these optics clearly resolved olfactory cilia and large subcellular organelles. The membrane currents in both intact neurons and isolated dendrites were studied using whole-cell patch-clamp methods (Hamill, Marty, Neher, Sakmann, and Sigworth, 1981). Odorant-induced conductance changes were studied using the resistive whole-cell method (Dionne, 1992). Currents were detected, amplified and filtered (at 10 khz) with an Axopatch amplifier (Axon Instruments, Inc., Foster City, CA), digitally recorded with a laboratory computer system (Indec Systems, Inc., Sunnyvale, CA), and stored on magnetic disk for off-line analysis. Data acquisition and analysis were performed with programs written in BASIC-23 in this laboratory. Patch electrodes were fabricated from Corning 8161 capillary tubing (Corning Glass, Inc., Corning, NY; WPI, Sarasota, FL) with a Brown-Flaming micropipette puller (Sutter Instrument Co., Novato, CA). All records shown have had the leak current subtracted; leak currents were estimated by averaging 16 or 32 hyperpolarizing pulses (25 mV) applied from the holding potential. Membrane capacitance and series resistance were estimated from capacitative transients. A complete description of the methods for cell preparation and data acquisition can be found elsewhere (Dionne, 1992; Dubin and Dionne, 1993).

Unless otherwise noted, compounds were applied by pressure ejection from a puffer pipet positioned near the dendrite or cell or by a rapid (1–2 s) bath exchange. Reversal potential measurements of affected currents or conductances were determined as described in Dubin and Dionne (1993).

All values with uncertainties are expressed as mean ± standard error of the mean with the number of measurements in parentheses. Values computed from several types of measurements are expressed similarly using standard rules for error propagation (Taylor, 1982).

Solutions

For the measurements reported here, cells were bathed in normal amphibian physiological saline (APS) and in modified APS that either was potassium-free or had low Cl^- or low Na^+. Both normal and zero-K^+ (Cs^+ substituted) amphibian intracellular salines (AIS) were employed. The compositions of all salines are given in Table I. In some experiments tetrodotoxin (TTX, 1 μM, Calbiochem Corp., La Jolla, CA) was included in the bathing solution to block fast transient Na^+ currents. The following agents, dissolved in extracellular salines as noted in the text, were used to pharmacologically characterize the currents: 4,4′-diisothiocyanatostilbene-2,2′-disulfonic acid (DIDS), niflumic acid, tetraethylammonium chloride (TEA-Cl), TEA-acetate, $BaCl_2$, $CdCl_2$, $NiCl_2$, diltiazem (racemic mixture), and amiloride. Niflumic acid was prepared as a 150 mM stock solution in absolute ethanol. DIDS was prepared as a 300 mM stock suspension in water and vortexed prior to dilution in the test salines. The pH of all solutions was adjusted to 7.4 before use. All compounds were obtained from Sigma Chemical Co. (St. Louis, MO) unless noted otherwise.

RESULTS

Intact neurons and isolated dendrites were dissociated from olfactory epithelia of adult aquatic salamanders (*Necturus maculosus*) (Fig. 1; see Methods). Isolated dendrites were identified by their characteristic morphology, resembling the dendrites on intact cells and including a cluster of olfactory cilia at one end (Fig. 1 *A*). In some cases the cilia were motile, waving slowly in a manner similar to the movement of cilia on some intact mudpuppy olfactory neurons. All the isolated dendrites used in this study appeared to have a normal complement of cilia. Olfactory neurons were one of two prominent ciliated cell types in these preparations. The other type was a large, roughly spherical cell with a tuft of several hundred cilia which beat synchro-

TABLE I

Composition of the Intracellular and Extracellular Salines

	NaCl	KCl	CsCl	$CaCl_2$	$CaSO_4$	$MgCl_2$	Na-ise	NMG
Extracellular salines								
APS	130	2.5	—	3	—	1	—	—
K-free APS	130	—	2.5	10	—	1	—	—
low-Cl APS	—	—	2.5	—	10	1	130	—
low-Na APS	—	2.5	—	3	—	1	—	130
	K-glu	KCl	CsCl	Cs-M	$MgSO_4$	$MgCl_2$	$CaCl_2$	K_4BAPTA
Intracellular salines								
AIS	90	25	—	—	—	3	0.483	1
Cs-AIS	—	—	25	102.5	—	3	0.483	1

All extracellular solutions contained (in mM) 10 hemi-NaHEPES, 5 glucose, and 5 Na-pyruvate (except low-Na APS) at pH 7.4. All intracellular solutions contained 10 hemi-NaHEPES at pH 7.4; the free Ca^{2+} concentration was 0.1 μM buffered by either 1 or 10 mM BAPTA. The results with both BAPTA concentrations were indistinguishable, and the data were pooled. Usually 3 mM Mg-ATP and 10 μM GTP were included in the intracellular solution. Abbrevations: APS, amphibian physiological saline; AIS, amphibian intracellular saline; Na-ise, Na-isethionate; NMG, *N*-methyl-D-glucamine; Cs-M, Cs-methanesulphonate; BAPTA, 1,2-bis(2-aminophenoxy) ethane *N,N,N'*-tetra-acetic acid.

nously and vigorously (Fig. 1 *C*). These are probably rounded-up respiratory cells (Trotier and MacLeod, 1986) which have also been termed "Medusa cells" (Maue and Dionne, 1988). The morphological differences between isolated dendrites and Medusa cells ensured that the two were not confused. In addition, the membrane conductances in Medusa cells differ from those in receptor neurons and isolated dendrites (see below).

Dendritic Action Potentials

By using whole-cell, current-clamp recording methods, action potentials could be elicited by small current pulses in isolated dendrites (Fig. 2). Typical action potentials

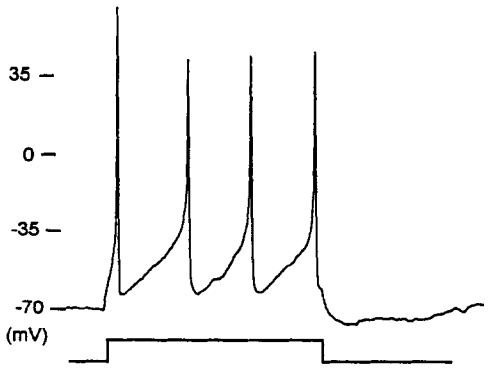

FIGURE 2. Action potentials in an isolated dendrite. Repetitive overshooting action potentials were elicited in current-clamp mode by a suprathreshold 20-pA, 400-ms depolarizing current pulse. The time course of the injected current is shown below the voltage trace. The resting potential of this dendrite was about −57 mV (recording condition: APS, AIS); for the trace shown it was held hyperpolarized with 8 pA. A hyperpolarizing bias current was ap-plied to most dendrites when testing for action potentials and in particular when K^+ currents were blocked with intracellular Cs^+. Repetitive firing, while not infrequently observed, was not common; most tests elicited a single action potential in response to a strong depolarizing current pulse.

had durations of 5–10 ms, a mean peak voltage of 17 ± 5 mV (n = 16), and small after-hyperpolarizations; they were indistinguishable from action potentials seen in intact neurons. The threshold for action potential generation was about −50 mV. For isolated dendrites, the input resistance averaged 1.9 ± 0.3 GΩ (n = 23) at −80 mV; under the same conditions, intact olfactory neurons had a mean input resistance of 1.6 ± 0.3 GΩ (n = 20). Isolated dendrites had only one-third the surface area of intact neurons as estimated from their membrane capacitance, C_{DEN} = 5.35 ± 0.27

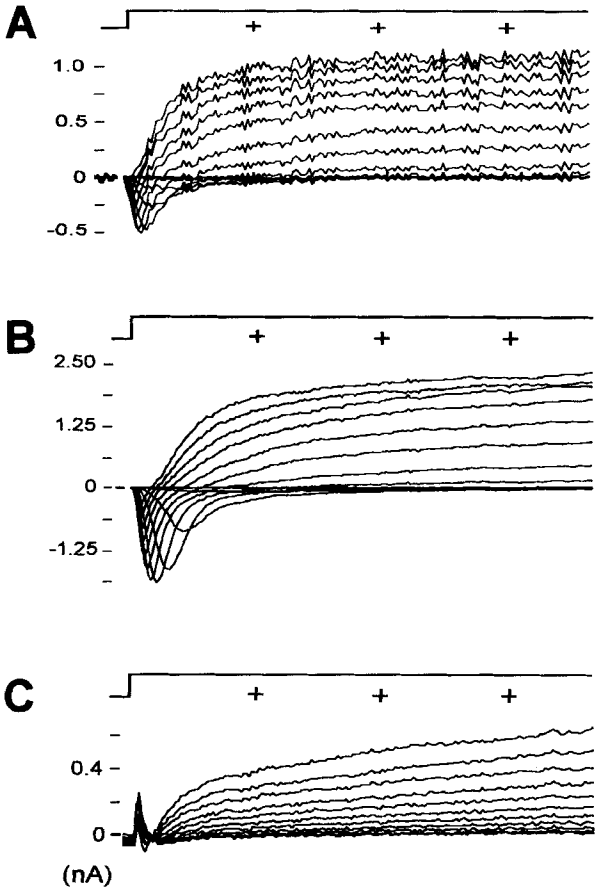

FIGURE 3. Voltage-activated currents. Families of currents activated by voltage steps of increasing magnitude are shown for (*A*) an isolated dendrite, (*B*) an intact neuron, and (*C*) a non-neuronal Medusa cell. The time course of the voltage steps is diagrammed at the top of each panel with cursors marking the time base at 5-ms intervals. Successive steps were applied at 400-ms intervals. The holding potentials between steps were −90 mV (*A* and *B*) and −70 mV (*C*); the test potentials ranged from −60 to +60 mV (*A* and *B*) and −40 to +60 mV (*C*), increasing in increments of 10 mV. For the dendrite and intact neuron, the family of currents reveals transient inward (negative) voltage-gated Na^+ currents and sustained outward (positive) currents that are carried by K^+ and Cl^-. For the Medusa cell, no transient inward currents were detected even with more hyperpolarized holding potentials, but outward currents (carried predominantly by K^+ and Cl^-) were found. Incompletely compensated capacitative transients were removed in *A* and *B* but not in *C*. Outward current density at +60 mV (pA/pF): +126 (*A*), +147 (*B*), +8 (*C*). Peak inward current density (pA/pF): −64 (*A*), −124 (*B*) (recording conditions: APS, AIS).

pF (n = 54) and C_{CELL} = 16.40 ± 0.35 pF (n = 89), respectively. By comparison, the average membrane capacitance of the non-neuronal Medusa cells was substantially larger than that of intact olfactory neurons (53.7 ± 9.1 pF; n = 7).

Dendritic Currents

Large amplitude, voltage-activated currents were detected in isolated olfactory dendrites using standard whole-cell recording techniques (Fig. 3 *A*). The currents

showed transient inward and sustained outward components. In some dendrites the peak inward current (observed at ~0 mV) exceeded 1 nA and the outward current at +60 mV exceeded 2 nA. The time course of the dendritic currents was similar to that of currents from intact olfactory neurons (Fig. 3 *B*), suggesting that the major voltage-gated conductances were similar in both. Below, we will show that the inward currents in isolated dendrites are primarily carried by Na^+ whereas the outward currents are carried by K^+ and Cl^-. The dendritic currents differed from those seen in Medusa cells (Fig. 3 *C*) where no action potentials could be elicited and where voltage pulses activated sustained outward K^+ and Cl^- currents but no transient inward currents.

Sodium current. Extracellular application of 1 μM TTX to isolated dendrites blocked overshooting action potentials and attenuated transient inward currents elicited by voltage pulses under voltage-clamp conditions (Fig. 4, *A* and *B*). Blockade of the inward current by TTX was fully reversed within minutes by washing with normal extracellular saline. Maximum peak inward currents in dendrites (-75.4 ± 5.3 pA/pF; $n = 32$) were similar to those elicited in intact cells (-68.3 ± 4.2 pA/pF; $n = 64$). The activation kinetics of the transient inward current in dendrites are shown in Fig. 4 *C*. Na^+ current activated with an apparent threshold of -45 ± 5 mV ($n = 28$), showed a maximum peak value at -8 ± 2 mV ($n = 30$), and appeared to reverse near +60 mV. Depolarizing prepulses inactivated the current (Fig. 4 *D*) with a half-inactivation potential of -59.5 ± 1.3 mV ($n = 24$). These parameters are similar to those of intact cells with the exception that the half-inactivation potential was 6 mV more depolarized in intact cells (-53.5 ± 1.3 mV; $P < 0.004$; $n = 37$). In low-Na APS, action potentials could not be elicited and the transient inward currents were absent. The time course of the transient current, its sensitivity to TTX, its requirement for extracellular Na^+, and the voltage dependence of its activation and inactivation kinetics all suggest that it is produced by prototypical voltage-gated Na^+ channels.

Potassium current. Both in isolated dendrites and in intact neurons, a part of the voltage-activated outward current was carried by K^+. When intracellular K^+ was replaced with Cs^+ which blocks all K^+ currents, average outward currents were reduced ~60% in dendrites and ~80% in intact cells. The outward current was also partially and reversibly attenuated when 10 mM TEA was applied extracellularly. In the isolated dendrites the fraction of outward current blocked by external TEA varied widely, ranging from 10% to 70% ($n = 4$); most of the remaining current could be blocked by DIDS and niflumic acid (see below). We believe this variability of the TEA-sensitive current accurately reflects the variability of the K^+ conductance in isolated dendrites; comparable data could not be obtained by blocking with internal Cs^+ because the experimental protocol did not allow measurement of the basal (unblocked) current.

The K^+ current density was estimated in isolated dendrites and somatic membrane to evaluate its distribution (Table II). Outward currents were measured at +60 mV either with high intracellular K^+ in the pipet (AIS; 15 dendrites, 33 intact cells) or with Cs^+ replacing K^+ (Cs-AIS; 26 dendrites, 31 intact cells). (See Table I for solutions.) To compensate for cell size, each current measurement was normalized using the capacitance of the cell or dendrite from which it was obtained, and the normalized measurements were averaged for each group. The average K^+ current

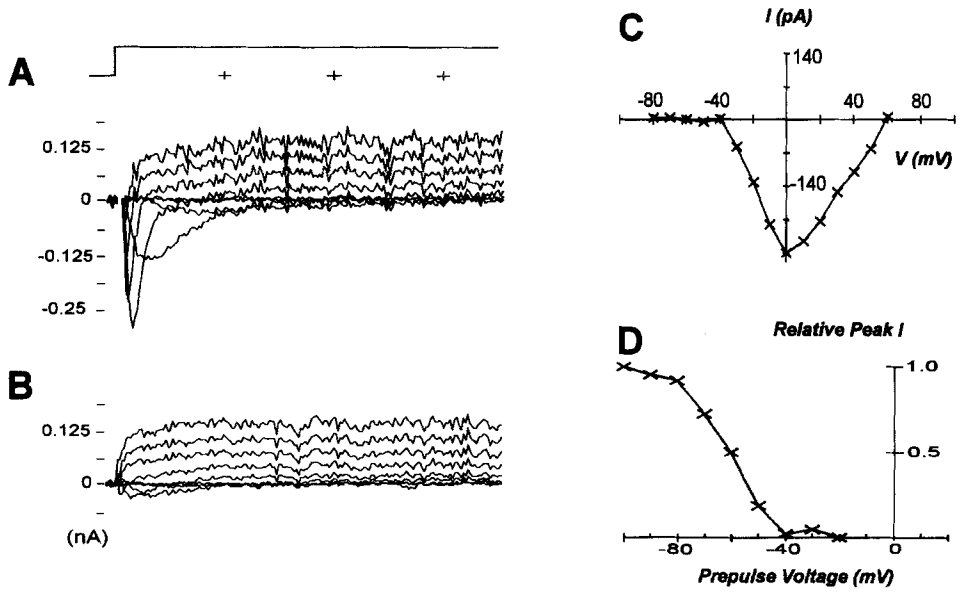

FIGURE 4. Na^+ currents in isolated dendrites. The data in this figure are from a single isolated dendrite bathed in K-free APS; the pipet contained Cs-AIS with 3 mM Mg-ATP and 10 μM GTP. (*A*) A family of current traces elicited by voltage steps from a holding potential of −90 mV with test potentials from −80 to +60 mV shown in 20-mV increments. The voltage-step profile is illustrated at the top of the panel with cursors marking the time base at 5-ms intervals. The traces reveal large transient inward (negative) currents maximally activated near 0 mV; at positive test potentials the currents were outward (positive) and sustained. (*B*) A family of current traces activated as in *A* but in the presence of 1 μM TTX. TTX nearly completely blocked the inward currents but had no effect on the outward currents. The time marks at the top of *A* correspond to 15 ms in this panel. The small TTX-insensitive inward current that remained may have been carried by Ca^{2+}; 0.1–1 mM Cd^{2+} with or without 200 μM Ni^{2+} blocked it by 27 ± 5% in dendrites (n = 4) and 36 ± 7% in intact cells (n = 7) (data not shown). (*C*) The peak inward current–voltage relation for the data in *A*. The peak current density at 0 mV was −67.1 pA/pF. (*D*) Steady-state inactivation data from the currents in *A*. Each of the voltage steps in *A* was held for 100 ms, then stepped to −20 mV to measure the fraction of Na^+ current that had not been inactivated. This fraction is plotted as a function of the initial voltage step potential. The half-inactivation voltage was −60 mV.

densities were defined as the difference in the mean normalized outward currents measured in the absence and presence of internal Cs^+. In isolated dendrites the average K^+ current density was I_{DEN} = 85.6 ± 19.5 pA/pF, while the value for intact cells was I_{CELL} = 95.1 ± 8.8 pA/pF. The large uncertainty in this value for dendrites reflects the variability mentioned above. These values were used with Eq. 1 to estimate the current density for the somatic membrane alone.

$$I_{SOMA} = (I_{CELL} C_{CELL} - I_{DEN} C_{DEN})/(C_{CELL} - C_{DEN}) \quad (1)$$

The predicted average K^+ current density in somatic membrane was 99.7 ± 17.5 pA/pF. This is comparable to the mean of 85.6 pA/pF from isolated dendrites, suggesting that *on average* the K^+ conductance has a fairly uniform density on somatic

TABLE II

K^+ and Cl^- Current densities

	I_K (pA/pF)	I_{Cl} (pA/pF)	C (pF)
Intact cells	95.1 ± 8.8	15.7 ± 2.8	16.40 ± 0.35
Isolated dendrites	85.6 ± 19.5	34.4 ± 9.7	5.35 ± 0.27
Soma (calculated)	99.7 ± 17.5	6.3 ± 2.2	11.05 ± 0.44

As described in the text, K^+ and Cl^- currents were measured in intact cells and isolated dendrites, normalized to the membrane capacitance, and used to calculate the current densities in somatic membrane alone. The average ciliated dendrite had 535 μm^2 of surface while the average intact cell had 1,640 μm^2 (assuming 1 $\mu F/cm^2$). Similar values (530 and 1,780 μm^2, respectively) would be expected for a typical mudpuppy olfactory neuron having the following dimensions: 20-μm diam spherical soma; 70-μm-long by 1.5-μm diam cylindrical dendrite; eight cylindrical cilia each 20 μm long by 0.4 μm diam.

and dendritic membrane. However, as noted above, wide variability was observed among individual cells.

Chloride current. Three-quarters of the voltage-activated outward current observed in isolated dendrites with Cs-AIS in the pipette (to block K^+ currents) was reversibly inhibited by the chloride channel blockers (CCBs), niflumic acid (300 μM) and DIDS (1 mM) (mean 76 ± 7% block; range 40–100%; $n = 12$). The CCB-sensitive current was activated quickly by voltage steps above −20 mV (see Fig. 7) and was sustained without inactivation for at least 1 s (data not shown). The outward current increased monotonically with voltage above 0 mV rather than showing N-shaped behavior, suggesting that it was not activated by Ca^{+2}. The CCB-sensitive current had a reversal potential similar to and dependent upon the Cl^- equilibrium potential (E_{Cl}) and insensitive to cation substitution, indicating that it was carried by Cl^- (Fig. 5). The reversal potential was estimated from the difference between whole-cell ramp-induced current–voltage curves elicited in the presence and absence

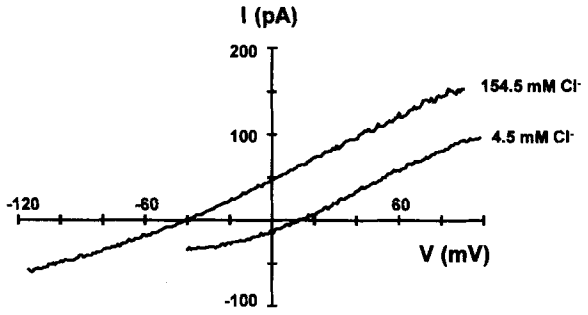

FIGURE 5. The reversal potential of the DIDS- and niflumic acid-sensitive current in isolated dendrites. The current-voltage relations for the CCB-sensitive current from two different isolated dendrites recorded in high and low chloride salines are shown. In 154.5 mM Cl^- saline (K-free APS/Cs-AIS; $E_{Cl} = -40$ mV), the CCB-sensitive current had a reversal potential of −39 mV. The reversal potential was +14 mV in a 4.5 mM Cl^- bath (low-Cl APS/Cs-AIS; $E_{Cl} = +49$ mV). Ramp current–voltage curves for isolated dendrites were measured in whole-cell mode, and the difference between currents recorded in the absence and presence of 1 mM DIDS plus 300 μM niflumic acid was plotted. The currents were activated by first stepping to +100 mV and holding for 100 ms while the Na^+ channels inactivated, then making a 75-ms ramp to −140 mV. The difference currents are shown over a subset of this range.

of 1 mM DIDS and 150–300 μM niflumic acid. Ramps were applied at 0.4-s intervals, and the control and block responses were acquired within seconds of one another, minimizing the possibility of ion redistribution. Block by the CCBs was rapid in onset, reversible and reproducible, indicating that the responses were not due to changes in the seal resistance. For cells bathed in 154.5 mM extracellular Cl^- (K-free APS), the reversal potential averaged -37 ± 4 mV ($n = 6$), not significantly different from E_{Cl} (-40 mV). The reversal potential of a dendrite bathed in low-Cl^- APS was 51 mV more positive ($+14$ mV) although not as positive as the calculated E_{Cl} ($+49$ mV).

The CCB-sensitive current was also seen in intact olfactory neurons where, similar to isolated dendrites, a shift of the reversal potential to $+10 \pm 2$ mV ($n = 5$) was observed when cells were bathed in low-Cl^- APS. In intact neurons the current was tested to determine if it was partly carried by cations; we measured its reversal potential in low-Na APS with AIS in the pipet, conditions which set E_{Cl} to -37 mV and the reversal potential for cations (assuming equal permeabilities for Na^+ and K^+) to -70 mV. Under these conditions, the reversal potential of the CCB-sensitive current was -25 ± 5 mV ($n = 3$). This value suggests that Cl^- is the major carrier of the CCB-sensitive current. Although the reversal potential was more positive than expected, the difference was opposite in direction from that predicted if cations had made a significant contribution to the blocked current. A fraction of intact olfactory neurons showed an anomalous response to the CCBs (see legend to Fig. 7) that may account for the discrepancy; even if this anomalous conductance were present, it would not affect our conclusion that Cl^- is the carrier of the CCB-sensitive current. Although our experimental protocol made it impossible to show reversible shifts of the reversal potential of the CCB-sensitive current in isolated dendrites following Cl^- exchange, our identification of Cl^- as the current carrier is strong. In isolated dendrites the CCB-sensitive current had the same temporal, voltage, and pharmacological properties as that observed in whole cells where the identification of Cl^- is more complete, and the CCB-sensitive current was present even when intracellular K^+ (the only other possible carrier of a sustained outward current) was replaced by Cs^+.

In situ, the value of E_{Cl} partially determines whether changes in the Cl^- conductance will be excitatory or inhibitory. Using an extracellular recording method, we estimated a Cl^- reversal potential of -45.5 ± 2.5 mV ($n = 11$) in dissociated, intact olfactory neurons bathed in APS (Fig. 6). To do this, the tips of recording pipettes were filled with normal APS for 1–2 mm and backfilled with APS containing 1 mM DIDS and 300 μM niflumic acid. The pipette was quickly sealed onto a dendritic knob or soma and voltage-ramp induced currents were recorded from on-cell membrane patches (see *inset*, Fig. 6). With normal APS in the pipette tip, the voltage ramp-currents were carried predominantly by K^+ and Cl^-. Within a minute the ramp current declined, presumably because the CCBs diffused to the membrane and blocked Cl^- current (no such decline was seen in the absence of CCBs). After collecting data from the same patch in the absence and presence of the blockers, we switched to current-clamp mode, applied suction to the pipette to obtain a whole-cell recording, and measured the initial zero-current resting potential. The average current–voltage curves in the absence and presence of the blockers crossed at a voltage which identified E_{Cl}. Assuming that the Cl^- channels were highly selective,

the estimated intracellular Cl^- concentration was 23.3 ± 2.5 mM (n = 11) when dissociation activities for ions in solution were taken into account.

The block of voltage-activated Cl^- currents in isolated dendrites and intact cells by both DIDS and niflumic acid was dose-dependent. Data for block by DIDS are shown in Fig. 7. Partial dose–response curves collected from three dendrites and five intact cells (each normalized to the block produced by 1 mM DIDS) were similar and are plotted together in Fig. 7 *B;* 50% block was produced by 44 ± 5 μM DIDS, and the Hill coefficient was 1.2 ± 0.2. The single isotherm shape of the dose–response curve for DIDS suggests that a single type of Cl^- channel underlies the voltage-gated Cl^-

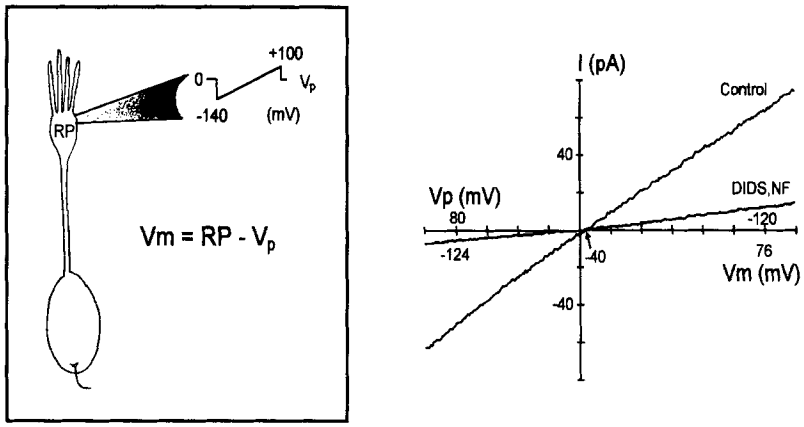

FIGURE 6. Estimation of E_{Cl} in olfactory receptor neurons. Voltage ramp-induced currents were recorded from a cell-attached patch formed on the dendritic knob of an intact olfactory neuron bathed in APS (*inset*). The control current was recorded just after obtaining a stable seal resistance and demonstrates the presence of voltage-activated conductances in the absence of any blockers. The trace marked DIDS, NF was recorded <2 min later, after block by the CCBs. The crossing voltage of the two traces was −4 mV pipet potential relative to the membrane potential. A membrane potential of −44 mV was then measured in whole-cell mode, indicating an actual reversal potential of −40 mV. The voltage axis is marked in both pipette potential (V_p) and membrane potential (V_m). The conductance of the patch under "control" conditions was ~550 pS; this declined to ~100 pS in the presence of the CCBs.

conductance. Niflumic acid produced similar effects with a half-maximal concentration of 10–30 μM (data not shown).

Cl^- current could be detected in membrane patches from the dendritic knob (see Fig. 6), demonstrating the presence of Cl^- channels in this region of the cell. To evaluate the distribution of the Cl^- conductance, Cl^- currents were measured in isolated dendrites and intact cells (Table II). The mean Cl^- current was defined as the difference between outward currents at +60 mV (using the voltage step protocol) measured in each cell or dendrite in the absence and presence of 1 mM DIDS, 300 μM niflumic acid, or both 1 mM DIDS and 150–300 μM niflumic acid. In all cases, Cs^+ replaced K^+ (Cs-AIS) in the pipette to block K^+ currents. The mean normalized Cl^- current in isolated dendrites was 34.4 ± 9.7 pA/pF (n = 12), and the value for intact cells was 15.7 ± 2.8 pA/pF (n = 13). Eq. 1 was used to estimate an average Cl^-

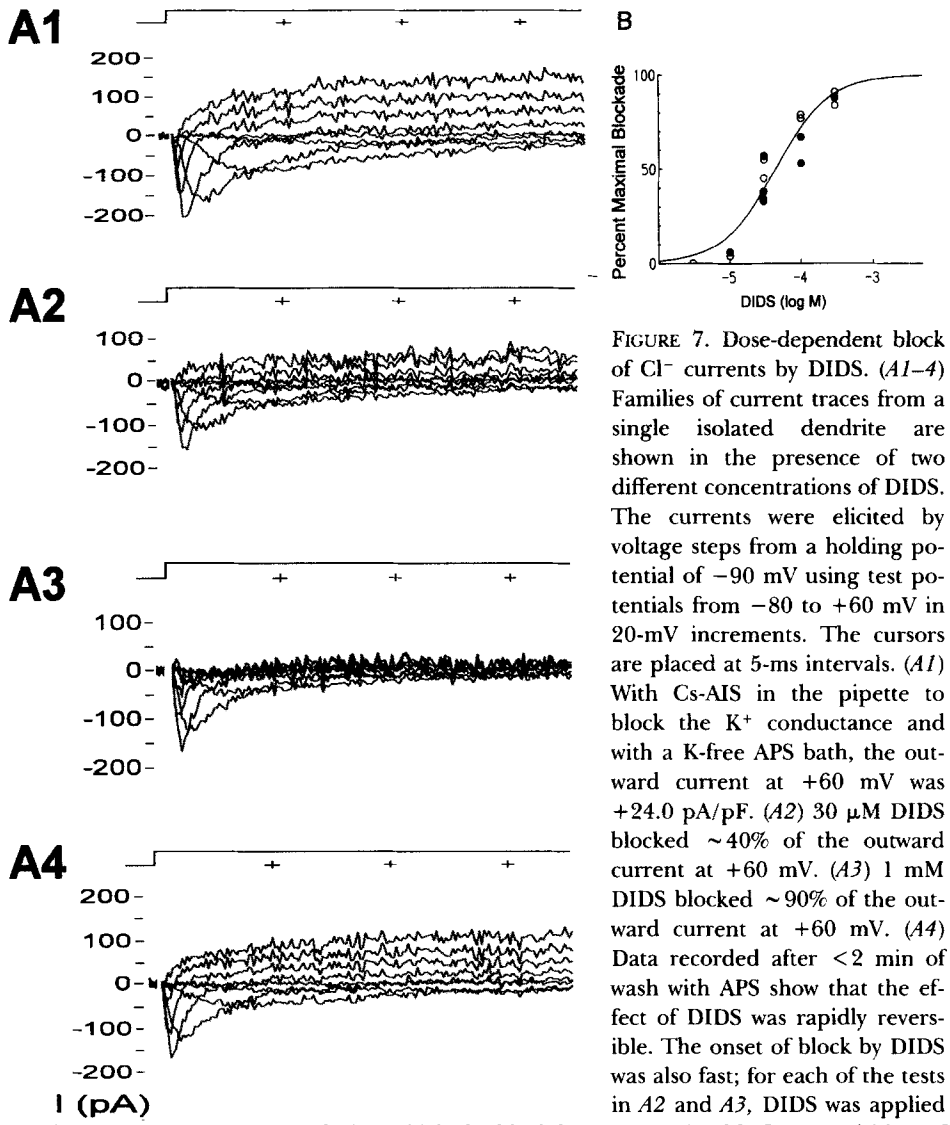

FIGURE 7. Dose-dependent block of Cl^- currents by DIDS. (*A1–4*) Families of current traces from a single isolated dendrite are shown in the presence of two different concentrations of DIDS. The currents were elicited by voltage steps from a holding potential of −90 mV using test potentials from −80 to +60 mV in 20-mV increments. The cursors are placed at 5-ms intervals. (*A1*) With Cs-AIS in the pipette to block the K^+ conductance and with a K-free APS bath, the outward current at +60 mV was +24.0 pA/pF. (*A2*) 30 μM DIDS blocked ~40% of the outward current at +60 mV. (*A3*) 1 mM DIDS blocked ~90% of the outward current at +60 mV. (*A4*) Data recorded after <2 min of wash with APS show that the effect of DIDS was rapidly reversible. The onset of block by DIDS was also fast; for each of the tests in *A2* and *A3*, DIDS was applied by puffer pipette for only 8.5 s during which the block became maximal before acquisition of the data. Furthermore, puffer application of CCBs to dendrites during continuous acquisition of voltage ramp-induced currents decreased ramps within 1–2 s (data not shown). (*B*) Dose dependence of the DIDS block in isolated dendrites and intact neurons. The percent block as a function of DIDS concentration is shown for isolated dendrites (●; three separate dendrites) and intact cells (○; five separate cells). The maximum for each dendrite or cell was defined as the block obtained with 1 mM DIDS; for dendrites, DIDS blocked 89 ± 3%; for intact cells, 79 ± 6%. The data were fit with Inplot (GraphPad, Inc., San Diego, CA) statistical software using a nonlinear regression and assuming a sigmoidal curve. The EC_{50} and Hill coefficient were adjustable parameters. About half of the intact cells responded with an anomalous increase in conductance to concentrations of DIDS or niflumic acid above 100 μM; these cells were not included in the data analysis. Recording condition: K-free APS/Cs-AIS.

current density for somatic membrane of 6.3 ± 2.2 pA/pF. This was <20% of the average density seen in isolated dendrites, suggesting that, in contrast to the K^+ conductance, most of the Cl^- conductance in mudpuppy olfactory neurons is located in the ciliated dendrite.

Odor Modulation of Currents in Isolated Dendrites

Isolated dendrites were tested for their ability to respond to the odorant taurine, a compound whose transduction mechanisms we have studied extensively in intact olfactory neurons (Dubin and Dionne, 1993). Current-clamp (as opposed to voltage-clamp) methods were routinely although not exclusively used to detect odor-

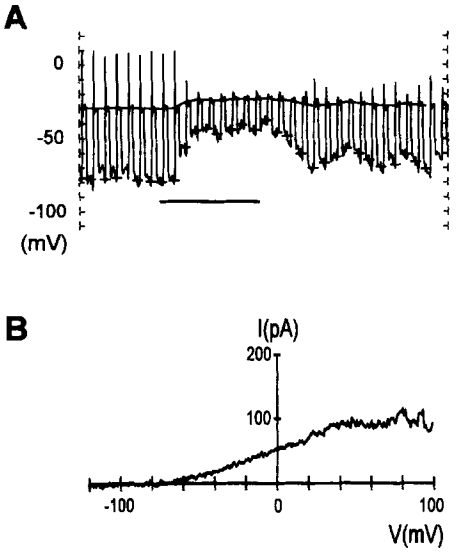

FIGURE 8. Responses of isolated dendrites to taurine. (*A*) In current-clamp mode, 400-ms-long depolarizing current pulses (40 pA) were injected at 1 Hz to monitor the membrane conductance of an isolated dendrite. The odorant taurine (10 μM, 8-s application marked by horizontal bar) increased the membrane conductance to 2,220 pS from a basal value of 800 pS, and caused the membrane to depolarize to −40 mV. Action potentials were elicited by each pulse prior to but not during exposure to taurine. The reversal potential of the taurine-induced conductance, estimated with the single-application method of Dubin and Dionne (1993), was −20 mV. The dendrite responded twice to taurine before washout occurred. After testing with taurine, the voltage-activated currents were examined in voltage-clamp mode; 1 mM DIDS blocked nearly all of the outward current (not shown), suggesting that the K^+ conductance was small. Control outward current at +60 mV was +58 pA/pF. (*B*). Taurine caused a decrease in the K^+ current in one isolated dendrite. The panel shows the difference current between ramps recorded in the absence and presence of 10 μM taurine. This taurine-inhibited current had a reversal potential near the K^+ equilibrium potential (E_K = −100 mV). Recording conditions for both panels: APS/AIS.

modulated conductances, since small changes in voltage were more readily observed than small changes in current. Taurine modulated the voltage-gated Cl^- and K^+ conductances in isolated dendrites with an incidence similar to that observed previously in intact cells. In nine isolated dendrites tested by puffer-application of taurine, three responded with an increase in the Cl^- conductance (Fig. 8 *A*), 1 with a decreased Cl^- conductance (data not shown), and 1 with a decreased K^+ current (Fig. 8 *B*). Most of these tests were conducted with 10 μM taurine, but responses were also obtained with 100 nM and 100 μM concentrations.

DISCUSSION

In vertebrate olfactory neurons, odors are transduced at the ciliated end of a single, thin dendrite. The dendrite (~1–2 μm in diameter) extends from the soma of the neuron to the surface of the epithelium, a distance that varies from 20 to 50 μm in most species and which can be up to 200 μm in salamanders such as the mudpuppy, *Necturus maculosus* (Graziadei and Graziadei, 1976). One consequence of the long, thin dendrite is that transduction processes which modulate neuronal excitability probably act primarily on the conductances of the ciliary and dendritic membranes at the apical end of the olfactory neuron. It has been proposed that odors induce a generator potential in these membranes which is propagated passively along the dendrite to the soma and axon hillock where action potentials are initiated (Getchell, 1973, 1986; Juge et al., 1979). Accordingly, an olfactory neuron is assumed to be electrotonically compact, allowing a local conductance change in the distal dendrite to produce a voltage change at the axon hillock without substantial decrement. If, on the other hand, dendritic membranes were capable of producing action potentials, a high degree of autonomy would be conferred on the dendritic knob to initiate and regulate neuronal activity. Here we show for the first time that isolated dendrites of mudpuppy olfactory neurons are capable of generating action potentials and demonstrate the presence in the ciliated dendrite of voltage-activated, odor-sensitive K^+ and Cl^- conductances. The ability of some odorants to modulate resting membrane conductances and the capacity of the dendritic membrane to generate action potentials near the site of odorant action may underlie the exquisite sensitivity of olfactory neurons to odors.

Na-dependent Action Potentials in Olfactory Dendrites

Dendrites isolated from mudpuppy olfactory neurons support TTX-sensitive, Na^+-dependent action potentials with a Na^+ conductance that appears to be distributed throughout the dendrite. The dendrites of some large, branched cortical neurons and cerebellar Purkinje cells also support action potentials (Llinas and Sugimori, 1980; Benardo, Masukawa, and Prince, 1982; Regehr, Konnerth, and Armstrong, 1992; Wong and Stewart, 1992), and action potentials can be initiated by small synaptic currents in apical dendritic regions (Regehr, Kehoe, Ascher, and Armstrong, 1993). We believe that dendritic action potentials in olfactory neurons reflect the situation in vivo since the alternative that Na^+ channels were found in the dendrites as a result of the dissociation procedures seems unlikely. Two scenarios can be envisioned whereby Na^+ channels might have redistributed to the dendrites; they are (*a*) that the Na^+ channels of isolated dendrites originated in fragments of somatic membrane torn from the soma during dissociation, or (*b*) that Na^+ channels redistributed into dendritic membrane from the soma following isolation of the cells but before the dendrite was severed. First, it is unlikely that the Na^+ channels originated in somatic membrane fragments isolated with the dendrites since the Na^+ current densities in isolated dendrites and intact cells were nearly equal. Second, the isolated dendrites were most probably separated from their somas during the mechanical steps of dissociation early in the procedure before any substantial redistribution of membrane proteins should occur.

Our data provide the first direct measurements of action potentials in olfactory dendrites. Whether olfactory dendrites in all species share this property or whether it is unique to the mudpuppy is unknown, but the potent enhancement in sensitivity which it provides (see below) suggests that this may be a generally utilized property. Studies conducted in frog olfactory epithelia by Getchell (1973) and Juge et al. (1979) and reviewed by Getchell (1986), using extracellular recordings, localized the spike initiation zone to the axon hillock and found no evidence for the existence of action potentials in the dendrites *in vivo;* however, action potentials would not have been detected in the dendritic membrane if, for instance, dendritic Na^+ channels had been inactivated. Steady state inactivation of Na^+ channels may be a means of odor modulation of cell excitability (Pun and Gesteland, 1991). We found a small but significant shift in the voltage required to half-inactivate Na^+ currents in isolated dendrites compared to that in intact cells. The mechanisms underlying this difference are currently under investigation. Although the insensitivity of neuronal activity to TTX applied to the mucosal side of the frog olfactory epithelium suggests that Na^+ channels in the apical membrane are not responsible for action potential generation (Frings et al., 1991), Na^+ channels located proximal to tight junctions would have been unaffected by TTX and could serve this role.

Odor Modulation of Cl^- and K^+ Conductances in Isolated Dendrites

Previously we demonstrated that odors can modulate the voltage-activated Cl^- conductance of mudpuppy olfactory neurons (Dubin and Dionne, 1993). Here we have shown that most of the voltage-activated Cl^- conductance appears to be confined to the dendritic and ciliary membranes where it remains sensitive to odor modulation. Hence a substantial fraction of Cl^- channels may be close enough to receptor sites to be readily affected by transduction processes.

We have also obtained the first estimate of the in situ value of the Cl^- equilibrium potential in olfactory neurons. The resting E_{Cl} in mudpuppy neurons is near -45 mV, a value slightly more depolarized than the threshold for generation of action potentials. Odors that decrease the Cl^- conductance would cause a cell to hyperpolarize due to an increasingly dominant K^+ resting conductance, resulting in inhibition; however, depending on the magnitude of the odor-response, cells might also show increased excitability since they would have a higher input resistance and require less depolarizing current to elicit an action potential. Odors that activate the Cl^- conductance would depolarize the cell and stimulate activity; however, for sensitive cells where odors caused an intense depolarization, inactivation of Na^+ channels would suppress electrical activity. Our earlier work has documented a variety of responses consistent with these varied expectations (Dubin and Dionne, 1993).

The specific effect on cell activity of modulating the Cl^- conductance must depend in part on the local distribution of the conductance and the type of Cl^- channels present. We found that most of the voltage-activated Cl^- conductance was confined to the ciliated dendrites where it could potentially be modulated by odor transduction processes; however, we have not determined whether the conductance is distributed uniformly in ciliary and dendritic membranes. Mudpuppy dendrites have a Cl^- conductance that is activated by membrane depolarization and which inactivates only

slowly during a sustained depolarizing voltage step. Given that odors exert different effects on the Cl^- conductance in different olfactory neurons, we consider it quite plausible that there may be different distributions in the dendrites and cilia of different cells. The channels can open at the resting potential, and their voltage-sensitivity may underlie the voltage-dependence of the Cl^- conductance described earlier (Dubin and Dionne, 1993). Furthermore, Cl^- channels activated by stimuli other than voltage have also been found in olfactory neurons; a Ca-activated Cl^- conductance has been described in frog, newt and tiger salamander (Kleene and Gesteland, 1991; Kleene, 1993; Kurahashi and Yau, 1993), where Ca^{2+} appears to enter the cell through cyclic nucleotide-gated cation channels. The Ca^{2+}-dependent Cl^- conductance can be a substantial component of the odor response (Kleene, 1993; Kurahashi and Yau, 1993). However, if E_{Cl} *in vivo* is similar to the value we have empirically obtained here (−45 mV), then the odor-induced response may not be as dramatic as those shown experimentally in which E_{Cl} was set at 0 mV (Anderson and Hamilton, 1987; Frings and Lindemann, 1988; Firestein et al., 1990; Kurahashi and Shibuya, 1990).

In contrast to the Cl^- conductance, the K^+ conductance in olfactory neurons appears to be distributed on average more uniformly. Yet, while prominent in all intact neurons, the K^+ conductance density in isolated dendrites varied considerably with some dendrites showing very low values. Low K^+ conductances have also been reported in olfactory dendrites from tiger salamander (Firestein et al., 1990; Lowe and Gold, 1991). Only the K^+ channels located near receptor sites should be affected by odor transduction. In many cells this will be a small fraction of the total number of K^+ channels, so that any effect of odors on electrical properties set by the resting K^+ conductance could be subtle. Regulation of the dendritic K^+ conductance by odors may account for the phenomenon we have termed "silent modulation" (Dionne, 1992) in which odor-induced effects on firing occur with no detectable change in the resting potential or input resistance of a cell. Since action potentials can be initiated in the dendrite and the dendrite has a high input impedance, even small changes in the dendritic K^+ conductance undetectable in recordings from the intact cell could have potent effects on firing. For example, reducing the apical K^+ conductance should destabilize the apical membrane potential locally and allow small currents from single ion channels in the dendrite to elicit large, transient changes in voltage which would alter firing.

Dendritic Action Potentials Enhance Chemosensitivity

Olfactory systems detect many odors at sub-picomolar concentrations and are able to achieve high sensitivity using low affinity receptors. How is reliable perception accomplished under these disparate conditions? Several features of odor transduction appear to be important. Three of these, second messenger cascades for signal amplification, a high membrane impedance to amplify small currents, and convergence of peripheral input in glomeruli have been reviewed recently (Kauer, 1991; Reed, 1992). Here we describe a fourth important feature, dendritic action potentials. The capacity to support dendritic action potentials allows small conductance changes in the apical region of the dendrite to reliably and directly modulate firing of olfactory neurons.

The processes of odor transduction overcome two major constraints. First, only the apical portion of a sensory neuron is exposed to odors, thus necessitating a process to locally transduce odorant binding into an electrical response; second, the likelihood of interaction is small between receptors and odorants at low concentrations, thus demanding high efficiency. A successful binding interaction first activates a second messenger cascade, effectively amplifying the signal (Pace, Hanski, Solomon, and Lancet, 1985; Boekhoff, Tareilus, Strotmann, and Breer, 1990). Since second messengers are diffusible compounds, their range of action is small, especially on a subsecond time scale; most of the effect mediated by second messengers probably occurs very near the apical end of the dendrite. The resulting actions modulate the activity of local ion channels, and it is this response that regulates neuronal firing. If action potentials were elicited *only* at the axon hillock, the odor-generated potentials would have to propagate passively from the dendritic ending to the soma in order to affect cell excitability. Reliable odor transduction would require a rapid and sizeable generator potential induced at the axon hillock by channel activity in the dendrite. Although this would be facilitated by a high input impedance, the sensitivity of the system would be reduced by the presence of somatic membrane which should shunt the generator currents. The sensitivity of olfactory neurons to odors would be greatly enhanced if action potentials were generated in the dendrite close to the location of the odor-modulated channels. This would minimize the effect of the somatic membrane shunt, at least on a short time scale, because the small surface area of the dendritic membrane could be charged and discharged rapidly by current from local odor-sensitive channels. In a similar way, dendritic action potentials in pyramidal cells increase the effectiveness of distal synaptic input in the motor cortex (Regehr et al., 1993). In this regard, the shape of the olfactory neuron contributes importantly to the requirement for high sensitivity, since its longitudinal resistance isolates small, transient currents in the chemosensitive and electrically active apical membrane from the capacitive load of the soma. This may be the selective pressure which has led to the extraordinary conservation of shape of olfactory neurons during evolution of the species.

Although action potentials can be elicited in olfactory dendrites, whether or not they propagate through the soma and on down the axon to reach the olfactory bulb is unclear. Dendritic action potentials may be quenched if the local currents which propagate them are too small to charge the somatic membrane. Even in this case, small odor-elicited apical currents would be amplified because the dendritic action potentials would more efficiently depolarize the soma and axon hillock, thus increasing the general level of excitability.

Our data here and in a previous study (Dubin and Dionne, 1993) show that odors modulate several different conductances in mudpuppy olfactory neurons. In particular both the K^+ and Cl^- conductances can be modulated by taurine in intact cells and isolated dendrites. Since these conductances are also the primary determinants of the resting potential, how can graded, odor-dependent effects on just the apically-located channels affect firing? The resting conductance is set by the K^+ and Cl^- channels which fluctuate randomly between open and closed states; moment-to-moment changes in the number of open channels will cause the membrane potential to vary between the Nernst values E_K and E_{Cl}. The high input impedance (because few

channels are open) and fluctuation in number of open channels cause olfactory neurons to have unstable resting potentials and to show spontaneous firing activity *in vivo* (Mathews, 1972; Getchell, 1973; Suzuki, 1978; Sicard, 1986; Baylin, 1979; Trotier and MacLeod, 1983; Frings et al., 1991). In a cell with a high input impedance, a brief depolarization of sufficient intensity would trigger an action potential. In olfactory neurons where the dendrite is capable of supporting action potentials, transduction integrity is preserved because the attenuation of fast transient voltage fluctuations that necessarily accompanies passive propagation is not a problem. Odor-induced changes in membrane conductance will alter both the variance of fluctuations in membrane potential and the input impedance of the cell. Thus, spontaneous fluctuations in the number of open K^+ and Cl^- channels at the apical end of the dendrite could provide the stimuli that make olfactory neurons fire, and odor-dependent modulation of either channel type would alter the frequency of firing.

Conclusions

Several studies have reported that the current through a single ion channel is capable of eliciting action potentials in olfactory neurons (Trotier, 1986; Maue and Dionne, 1987; Frings and Lindemann, 1988; Lynch and Barry, 1989). Such exquisite sensitivity to small currents may be necessary to provide reliable odor transduction. In mudpuppy, where we have shown for the first time that dendritic membranes have the capacity to generate action potentials, the apical ending can act with especially high efficiency to control and modulate neuronal firing. A large number of channel types have been identified in olfactory neurons (Anholt, 1989), but only a few studies have examined their location in the cell (Nakamura and Gold, 1987; Kurahashi, 1989; Firestein et al., 1991*b;* Frings et al., 1991; Lowe and Gold, 1991) or their sensitivity to odors (Firestein and Werblin, 1989; Firestein et al., 1991*b;* Michel et al., 1991; Dubin and Dionne, 1993). The Cl^- and K^+ conductances in mudpuppy olfactory dendrites are regulated by odors, and modulation of these conductances can affect firing in a manner that mimics transduction in the intact cell. These effects appear to constitute a sensitive and novel form of odor transduction. The second messenger pathways that couple odor binding to modulation of these specific conductances are still unknown, but our data suggest there may be several such pathways. Although all the isolated dendrites we studied had both K^+ and Cl^- conductances, taurine (which can modulate both) seldom affected both in the same cell or isolated dendrite. Apparently taurine (and possibly other odors) can activate different transduction pathways in different cells. A diverse mixture of transduction mechanisms may be necessary to produce the complex pattern of electrical activity that encodes the characteristics of an odor.

We thank Drs. Sue Kinnamon and Steven Kleene for critically reading the manuscript, Dr. Harvey Karten and Lance Washington for their help with the photography of isolated cells, and Dr. Tristram Bahnson, Elise Lamar, and Michael Deiner for helpful discussions during the course of this work and comments on the manuscript.

This work was supported by grant R01 DC-000256 from the National Institutes of Health.

Original version received 22 March 1993 and accepted version received 29 October 1993.

REFERENCES

Anderson, P. A. V. and K. A. Hamilton. 1987. Intracellular recordings from isolated salamander olfactory receptor neurons. *Neuroscience.* 21:167–173.

Anholt, R. R. 1989. Molecular physiology of olfaction. *American Journal of Physiology.* 257:C1043–C1054.

Baylin, F. 1979. Temporal patterns and selectivity in the unitary responses of olfactory receptors in the tiger salamander to odor stimulation. *Journal of General Physiology.* 74:17–36.

Benardo, L. S., L. M. Masukawa, and D. A. Prince. 1982. Electrophysiology of isolated hippocampal pyramidal dendrites. *Journal of Neuroscience.* 2:1614–1622.

Boekhoff, I., E. Tareilus, J. Strotmann, and H. Breer. 1990. Rapid activation of alternative second messenger pathways in olfactory cilia from rats by different odorants. *The EMBO Journal.* 9:2453–2458.

Dionne, V. E. 1992. Chemosensory responses in isolated olfactory receptor neurons from *Necturus maculosus*. *Journal of General Physiology.* 99:415–433.

Dubin, A. E., and V. E. Dionne. 1993. Modulation of Cl^-, K^+, and nonselective cation conductances by taurine in olfactory receptor neurons of the mudpuppy *Necturus maculosus*. *Journal of General Physiology.* 101:469–485.

Firestein, S., B. Darrow, and G. M. Shepherd. 1991*a*. Activation of the sensory current in salamander olfactory receptor neurons depends on a G protein-mediated cAMP second messenger system. *Neuron.* 6:825–835.

Firestein, S., G. M. Shepherd, and F. S. Werblin. 1990. Time course of the membrane current underlying sensory transduction in salamander olfactory receptor neurones. *Journal of Physiology.* 430:135–158.

Firestein, S., and F. Werblin. 1989. Odor-induced membrane currents in vertebrate olfactory receptor neurons. *Science.* 244:79–82.

Firestein, S., F. Zufall, and G. M. Shepherd. 1991*b*. Single odor-sensitive channels in olfactory receptor neurons are also gated by cyclic nucleotides. *The Journal of Neuroscience.* 11:3565–3572.

Frings, S., S. Benz, and B. Lindemann. 1991. Current recording from sensory cilia of olfactory receptor cells in situ. II. Role of mucosal Na^+, K^+, and Ca^{2+} ions. *Journal of General Physiology.* 97:725–747.

Frings, S., and B. Lindemann. 1988. Odorant response of isolated olfactory receptor cells is blocked by amiloride. *Journal of Membrane Biology.* 105:233–243.

Getchell, T. V. 1973. Analysis of unitary spikes recorded extracellularly from frog olfactory receptor cells and axons. *Journal of Physiology.* 234:533–551.

Getchell, T. V. 1986. Functional properties of vertebrate olfactory receptor neurons. *Physiological Reviews.* 66:772–818.

Graziadei, P. P. C., and G. A. M. Graziadei. 1976. Olfactory epithelium of *Necturus maculosus* and *Ambystoma tigrinum*. *Journal of Neurocytology.* 5:11–32.

Hamill, O. P., A. Marty, E. Neher, B. Sakmann, and F. S. Sigworth. 1981. Improved patch-clamp techniques for high resolution current recording from cells and cell-free membrane patches. *Pflugers Archives.* 391:85–100.

Juge, A., A. Holley, and J. C. Delaleu. 1979. Olfactory receptor cell activity under electrical polarization of the nasal mucosa in the frog. *Journal de Physiologie.* 75:919–927.

Kauer, J. S. 1991. Contributions of topography and parallel processing to odor coding in the vertebrate olfactory pathway. *Trends in Neurosciences.* 14:79–85.

Kleene, S. J. 1993. Origin of the chloride current in olfactory transduction. *Neuron.* 11:123–132.

Kleene, S. J., and R. C. Gesteland. 1991. Calcium-activated chloride conductance in frog olfactory cilia. *Journal of Neuroscience.* 11:3624–3629.

Kolesnikov, S. S., A. B. Zhainazarov, and A. V. Kosolapov. 1990. Cyclic nucleotide-activated channels in the frog olfactory receptor plasma membrane. *FEBS Letters.* 266:96–98.

Kurahashi, T. 1989. Activation by odorants of cation-selective conductance in the olfactory receptor cell isolated from the newt. *Journal of Physiology.* 419:177–192.

Kurahashi, T., and T. Shibuya. 1990. Ca^{2+}-dependent adaptive properties in the solitary olfactory receptor cell of the newt. *Brain Research.* 515:261–268.

Kurahashi, T., and K.-W. Yau. 1993. Co-existence of cationic and chloride components in odorant-induced current of vertebrate olfactory receptor cells. *Nature.* 363:71–74.

Llinas, R., and M. Sugimori. 1980. Electrophysiological properties of in vitro Purkinje cell somata in mammalian cerebellar slices. *Journal of Physiology.* 305:171–195.

Lowe, G., and G. H. Gold. 1991. The spatial distributions of odorant sensitivity and odorant-induced currents in salamander olfactory receptor cells. *Journal of Physiology.* 442:147–168.

Lynch, J. W., and P. H. Barry. 1989. Action potentials initiated by single channels opening in a small neuron (rat olfactory receptor). *Biophysical Journal.* 55:755–768.

Lynch, J. W., and P. H. Barry. 1991. Properties of transient K^+ currents and underlying single K^+ channels in rat olfactory receptor neurons. *Journal of General Physiology.* 97:1043–1072.

Mathews, D. F. 1972. Response patterns of single neurons in the tortoise olfactory epithelium and olfactory bulb. *Journal of General Physiology.* 60:166–180.

Maue, R. A., and V. E. Dionne. 1987. Patch-clamp studies of isolated mouse olfactory receptor neurons. *Journal of General Physiology.* 90:95–125.

Maue, R. A., and V. E. Dionne. 1988. Membrane properties of isolated olfactory receptor neurons. *In* Molecular Neurobiology of the Olfactory System. F. L. Margolis and T. V. Getchell, Plenum Publishing Corporation, New York. 143–158.

McClintock, T. S., and B. W. Ache. 1989. Histamine directly gates a chloride channel in lobster olfactory receptor neurons. *Proceedings of the National Academy of Science.* 86:8137–8141.

Michel, W. C., T. S. McClintock, and B. W. Ache. 1991. Inhibition of lobster olfactory receptor cells by an odor-activated potassium conductance. *Journal of Neurophysiology.* 65:446–453.

Miyamoto, T., D. Restrepo, and J. H. Teeter. 1992. Voltage-dependent and odorant-regulated currents in isolated olfactory receptor neurons of the channel catfish. *Journal of General Physiology.* 99:505–530.

Nakamura, T., and G. H. Gold. 1987. A cyclic nucleotide-gated conductance in olfactory receptor cilia. *Nature* 325:442–444.

Pace, U., E. Hanski, Y. Solomon, and D. Lancet. 1985. Odorant-sensitive adenylate cyclase may mediate olfactory reception. *Nature.* 316:255–258.

Pun, R. Y., and R. C. Gesteland. 1991. Somatic sodium channels of frog olfactory receptor neurones are inactivated at rest. *Pflügers Archives.* 418:504–511.

Rajendra, S., J. W. Lynch, and P. H. Barry. 1992. An analysis of Na^+ currents in rat olfactory receptor neurons. *Pflügers Archives* 420:342–346.

Reed, R. R. 1992. Signaling pathways in odorant detection. *Neuron.* 8:205–209.

Regehr, W., J. Kehoe, P. Ascher, and C. Armstrong. 1993. Synaptically triggered action potentials in dendrites. *Neuron.* 11:145–151.

Regehr, W. G., A. Konnerth, and C. M. Armstrong. 1992. Sodium action potentials in the dendrites of cerebellar Purkinje cells. *Proceedings of the National Academy of Science.* 89:5492–5496.

Restrepo, D., T. Miyamoto, B. P. Bryant, and J. H. Teeter. 1990. Odor stimuli trigger influx of calcium into olfactory neurons of the channel catfish. *Science.* 249:1166–1168.

Sicard, G. 1986. Electrophysiological recordings from olfactory receptor cells in adult mice. *Brain Research.* 397:405–408.

Suzuki, N. 1978. Effects of different ionic environments on the responses of single olfactory receptors in the lamprey. *Comparative Biochemistry and Physiology [A].* 61:461–467.

Taylor, J. R. 1982. An Introduction to Error Analysis. The Study of Uncertainties in Physical Measurements. University Science Books, Mill Valley, CA.

Trotier, D. 1986. A patch-clamp analysis of membrane currents in salamander olfactory receptor cells. *Pflügers Archives.* 407:589–595.

Trotier, D., and P. MacLeod. 1983. Intracellular recordings from salamander olfactory receptor cells. *Brain Research.* 268:225–237.

Trotier, D., and P. MacLeod. 1986. Intracellular recordings from salamander olfactory supporting cells. *Brain Research.* 374:205–211.

Wong, R. K., and M. Stewart. 1992. Different firing patterns generated in dendrites and somata of CA1 pyramidal neurones in guinea-pig hippocampus. *Journal of Physiology.* 457:675–687.

Zufall, F., S. Firestein, and G. M. Shepherd. 1991. Analysis of single cyclic nucleotide-gated channels in olfactory receptor cells. *Journal of Neuroscience.* 11:3573–3580.